

Sesquiterpenes from an Egyptian Herbal Medicine, *Pulicaria undulata*, with Inhibitory Effects on Nitric Oxide Production in RAW264.7 Macrophage Cells

Mohamed-Elamir F. Hegazy,^{a,b} Hisashi Matsuda,^a Seikou Nakamura,^a Mikuko Yabe,^a Tomoko Matsumoto,^a and Masayuki Yoshikawa^{*a}

^aKyoto Pharmaceutical University; Misasagi, Yamashina-ku, Kyoto 607–8412, Japan; and ^bChemistry of Medicinal Plants Department, and Center of Excellence for Advanced Sciences, National Research Centre; El-Tahrir St., Dokki, Giza 12622, Egypt.

Received November 17, 2011; accepted December 20, 2011; published online January 6, 2012

The methylene chloride–methanol (1 : 1) extract from the air-dried aerial parts of wild *Pulicaria undulata* collected in North Sinia, Egypt, showed inhibitory effects on lipopolysaccharide (LPS)-induced production of nitric oxide (NO) in RAW264.7 macrophages. From the extract, three new sesquiterpenes named 5 α -hydroperoxyivalin, 8-*epi*-xanthanol, and 8-*epi*-isoxanthanol were isolated together with four known sesquiterpenes. The structure of each new sesquiterpenes was determined on the basis of physicochemical and chemical evidence. In addition, all the sesquiterpenoids significantly inhibited the production of NO. Ivalin (IC₅₀=2.0 μ M) and 2 α -hydroxyalantolactone (1.8 μ M) showed particularly strong inhibitory effects, but had strong cytotoxic effects as well. Furthermore, ivalin and 2 α -hydroxyalantolactone concentration-dependently reduced inducible NO synthase (iNOS) protein levels in RAW264.7 cells.

Key words *Pulicaria undulata*; sesquiterpenoid; nitric oxide production inhibitor; RAW264.7 cell; Compositae

The genus *Pulicaria*, belonging to the tribe *Inuleae* of the Compositae family, consists of 100 species with a distribution from Europe to North Africa and Asia, particularly centered around the Mediterranean.¹⁾ Phytochemical studies on *Pulicaria* species have yielded several flavonoids and terpenoids, including sesquiterpenoids and diterpenoids. Most importantly, a number of compounds from *Pulicaria* species have been found to possess potent bioactivities, and could be promising candidates for the development of potential drugs and value-added products.²⁾ *Pulicaria undulata* (L.) KOSTEL [syn. *P. crispa* (FORSSK.) BENTH. et HOOK. f., *Francoeuria crispa* (FORSSK.) CASS.] is an annual herb or sometimes a perennial sub shrub, producing small bright yellow flower. Known in Egypt as Dethdath, it is commonly used in traditional herbal medicines to treat inflammation, as an insect repellent, and even as a herbal tea.³⁾

The inorganic free radical nitric oxide (NO) has been implicated in physiological and pathological processes such as vasodilation, nonspecific host defense, ischemia-reperfusion

injury, and chronic or acute inflammation. NO is produced by the oxidation of L-arginine catalyzed by NO synthase (NOS). In the NOS family, inducible NOS (iNOS) is particularly well known to be involved in the pathological overproduction of NO. Chronic inflammation also contributes substantially to environmental carcinogenesis. Various infectious diseases and physical, chemical, and immunological factors participate in inflammation-related carcinogenesis. Under inflammatory conditions, reactive oxygen and nitrogen species are generated from inflammatory and epithelial cells, and so the suppression of signaling molecules for iNOS expression may have great potential for the prevention and treatment of inflammation-associated carcinogenesis.^{4–7)}

In the present study, the methylene chloride–methanol (1 : 1) extract from the air-dried aerial parts of wild *P. undulata* collected in North Sinia, Egypt, was found to have inhibitory effects on LPS-induced NO production in RAW264.7 macrophages. Furthermore, we examined the inhibitory effects of all isolated constituents on NO production induced by lipopoly-

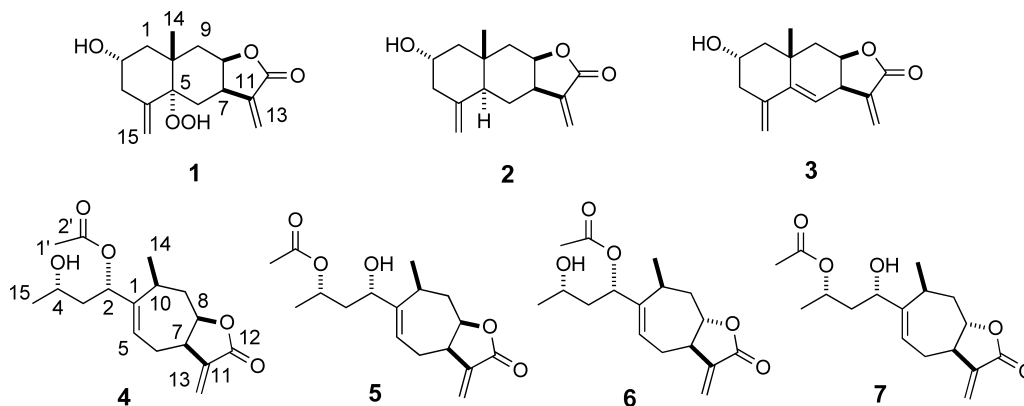


Fig. 1. Structures of the Compounds Isolated from *Pulicaria undulata*

* To whom correspondence should be addressed. e-mail: myoshika@mb.kyoto-phu.ac.jp

saccharide (LPS). In this paper, we describe the isolation and structural elucidation of the new constituents (**1**, **4**, **5**) and the inhibitory effects of constituents from the dried aerial parts of *P. undulate*.

Results and Discussion

Isolation and Structural Elucidation The methylene-chloride (CH₂Cl₂)–methanol (MeOH) (1:1) extract (6.77%) of the air-dried aerial parts of *P. undulate* inhibited production of NO in LPS-simulated RAW264.7 cells (IC₅₀=7.5 μg/mL).⁸ To clarify its active components, the extract was subjected to normal and reverse phase chromatography to afford three new compounds named 5α-hydroperoxyivalin (**1**, 0.0004%), 8-*epi*-xanthanol (**4**, 0.0013%), and 8-*epi*-isoxanthanol (**5**, 0.0022%) together with four known sesquiterpenoids, ivalin (**2**, 0.0012%),^{9,10} 2α-hydroxyalantolactone (**3**, 0.017%),¹¹ xanthanol (**6**, 0.0009%),^{12,13} and isoxanthanol (**7**, 0.0036%).^{12,13}

5α-Hydroperoxyivalin (**1**) was obtained as colorless needles with a positive optical rotation ($[\alpha]_D^{25} +22.0^\circ$ in MeOH). Its IR spectrum showed absorption bands at 3450, 1735 and 1650 cm⁻¹ ascribable to hydroxyl, γ-lactone and olefin functions. Positive-ion fast atom bombardment (FAB)-MS indicated a quasimolecular ion peak at *m/z* 303 (M+Na)⁺, and high-resolution (HR)-FAB-MS revealed the molecular formula C₁₅H₂₀O₅. The ¹H-NMR (CD₃OD) and ¹³C-NMR (Table 1) spectra of **1**, which were assigned based on NMR experiments,¹⁴ showed signals assignable to a methyl [δ 0.97 (3H, s, H₃-14)], two methines with an oxygen function [δ 3.76 (1H, m, H-2), 4.59 (1H, ddd, *J*=1.3, 5.5, 10.3 Hz, H-8)], four olefinic protons [δ 4.79, 5.09 (1H each, both brs, H₂-15), 5.70, 6.07

(1H each, both brs, H₂-13)], and a carbonyl carbon (δ_C 172.5, C-12). The proton and carbon signals of **1** in the ¹H- and ¹³C-NMR spectra resembled those of ivalin (**2**),^{9,10} except for the signals around the 5-position. Double quantum filter correlation spectroscopy (DQF COSY) indicated the presence of partial structures (written in bold in Fig. 2), and heteronuclear multiple bond connectivity spectroscopy (HMBC) revealed long-range correlations between the following protons and carbons: H-1 and C-2; H-6 and C-5, 7; H-7 and C-11; H-13 and C-12; H-14 and C-1, 5, 9; H-15 and C-5. These results supported that **1** was an alantolactone derivative with a hydroperoxyl moiety. Next, nuclear Overhauser enhancement spectroscopy (NOESY) revealed NOE correlations between the following proton pairs: H-1β and H-2, H₃-14; H-2 and H₃-14; H-6α and H-7; H-6β and H₃-14; H-7 and H-8 (Fig. 2). Finally, the stereostructure of **1** was characterized by a single crystal X-ray crystallographic analysis. The ORTEP representation of the X-ray structure is presented in Fig. 3. On the basis of this evidence, the structure of 5α-hydroperoxyivalin (**1**) was characterized as shown.

8-*epi*-Xanthanol (**4**) and 8-*epi*-isoxanthanol (**5**) were isolated as colorless needles with negative optical rotation (**4**: $[\alpha]_D^{25} -15.0^\circ$; **5**: $[\alpha]_D^{25} -22.0^\circ$ in MeOH). Their IR spectra showed absorption bands assignable to hydroxyl, γ-lactone, acetoxy and olefin functions (**4**, **5**: 3450, 1738, 1732, 1652 cm⁻¹). Chemical ionization (CI)-MS revealed a common quasimolecular ion peak at *m/z* 309 (M+H)⁺ and the molecular formula C₁₇H₂₅O₅ was determined by HR-CI-MS. The proton and carbon signals in the ¹H- and ¹³C-NMR spectra of **4** and **5** were very similar to those of xanthanol (**6**)^{12,13} and isoxanthanol

Table 1. ¹H- (600 MHz, **1**: CD₃OD, **4**, **5**: CDCl₃) and ¹³C- (150 MHz, **1**: CD₃OD, **4**, **5**: CDCl₃) NMR Data of **1**, **4**, and **5**

Position	1		4		5	
	δ_H (<i>J</i> in Hz)	δ_C	δ_H (<i>J</i> in Hz)	δ_C	δ_H (<i>J</i> in Hz)	δ_C
1	1.43 m ^{a)} 1.66 dd (11.6, 11.6)	45.0	—	145.2	—	147.7
2	3.76 m	67.4	5.10 dd (4.8, 8.9)	76.3	4.04 dd (5.5, 8.2)	73.4
3	2.44 m 2.55 dd (11.6, 11.6)	42.4	1.67 m 1.90 m	43.5	1.67 m 1.92 m	42.1
4	—	147.2	3.81 m	65.9	4.91 m	69.3
5	—	84.6	5.84 dd (5.5, 8.9)	124.1	5.69 dd (6.2, 8.9)	122.3
6	1.42 dd (2.1, 14.0) ^{a)} 2.33 dd (6.8, 14.0)	29.0	2.28 ddd (4.8, 8.9, 14.5) 2.43 m	26.2	2.27 ddd (4.8, 8.9, 15.5) 2.39 m	26.0
7	3.36 m	38.8	3.29 m	41.5	3.31 m	41.4
8	4.59 ddd (1.3, 5.5, 10.3)	78.8	4.57 ddd (2.7, 10.0, 12.3)	78.9	4.57 ddd (2.7, 11.0, 12.3)	79.1
9	1.87 dd (1.3, 14.0) 1.94 dd (5.5, 14.0)	36.7	1.81 m 2.03 m	36.9	1.79 m 2.03 ddd (2.7, 4.1, 12.3)	37.0
10	—	37.9	2.62 m	34.0	2.56 m	32.9
11	—	143.7	—	138.6	—	138.7
12	—	172.5	—	169.7	—	170.3
13	5.70 s like 6.07 s like	121.1	5.51 d (2.7) 6.25 d (2.7)	122.9	5.49 d (2.7) 6.22 d (2.7)	122.2
14	0.97 s	24.2	1.12 d (7.5)	21.5	1.14 d (6.9)	22.1
15	4.79 s like 5.09 s like	113.9	1.21 d (6.2)	23.7	1.23 d (6.2)	20.3
1'	—	—	2.01 s	21.6	2.00 s	21.5
2'	—	—	—	170.4	—	170.7

a) Overlapping signals.

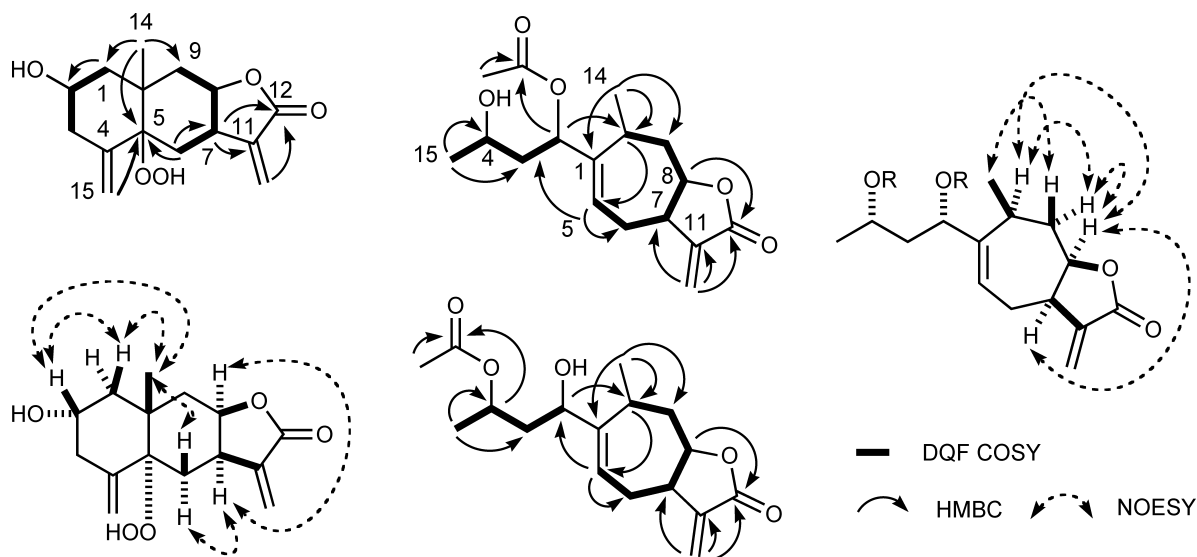


Fig. 2. Significant DQF COSY, HMBC, and NOE Correlations 1, 4, and 5

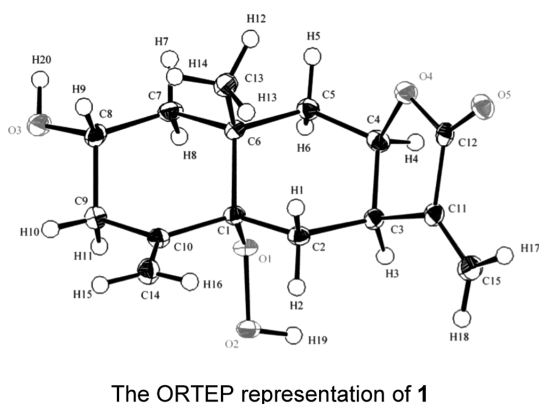


Fig. 3. ORTEP Representation of **1**

(**7**),^{12,13} respectively, except for the signals around the 8-position. The ¹H-NMR (CDCl₃) and ¹³C-NMR (Table 2) spectra, which were assigned based on results of various NMR experiments,¹⁴ showed signals due to three methyls [**4**: δ 1.12 (3H, d, *J*=7.5 Hz, H₃-14), 1.21 (3H, d, *J*=6.2 Hz, H₃-15), 2.01 (3H, s, H₃-1'); **5**: δ 1.14 (3H, d, *J*=6.9 Hz, H₃-14), 1.23 (3H, d, *J*=6.2 Hz, H₃-15), 2.00 (3H, s, H₃-1')], three methines with an oxygen function [**4**: δ 3.81 (1H, m, H-4), 4.57 (1H, ddd, *J*=2.7, 10.0, 12.3 Hz, H-8), 5.10 (1H, dd, *J*=4.8, 8.9 Hz, H-2); **5**: δ 4.04 (1H, dd, *J*=5.5, 8.2 Hz, H-2), 4.57 (1H, ddd, *J*=2.7, 11.0, 12.3 Hz, H-8), 4.91 (1H, m, H-4)], and three olefinic protons [**4**: δ 5.51, 6.25 (1H each, both d, *J*=2.7 Hz, H₂-13), 5.84 (1H, dd, *J*=5.5, 8.9 Hz, H-5); **5**: δ 5.49, 6.22 (1H each, both d, *J*=2.7 Hz, H₂-13), 5.69 (1H, dd, *J*=6.2, 8.9 Hz, H-5)]. As shown in Fig. 2, the DQF COSY experiments indicated the presence of partial structures (written in bold), and in the HMBC experiments, long-range correlations were observed between the following protons and carbons: **4**: H-2 and C-10, 2'; H-5 and C-2, 6; H-8 and C-12; H-10 and C-5; H-13 and C-7, 11, 12; H-14 and C-1, 9, 10; H-15 and C-3, 4; H-1' and C-2'; **5**: H-2 and C-10; H-4 and C-2'; H-5 and C-2, 6; H-8 and C-12; H-10 and C-5; H-13 and C-7, 11, 12; H-14 and C-1, 9, 10; H-15 and C-3, 4; H-1' and C-2'. Next, the relative stereostructures of the 7-, 8- and 10-positions in **4** and **5** were characterized

by NOESY experiments, which showed NOE correlations between the following proton pairs: H-7 and H-8; H-8 and H-9_α, H-10; H-9_α and H-10; H-9_β and H₃-14. In addition, it was reported that the absolute stereostructures of compounds with an α-methylene-γ-lactone moiety such as xanthanolides were determined based on circular dichroic (CD) spectra.^{15,16} Therefore, the absolute configurations of the 8-position on **4** and **5** were confirmed from CD spectra. Namely, the CD spectra of xanthanol (**6**) and isoxanthanol (**7**) with the 7*R* and 8*S* configurations showed positive Cotton effects at 254 nm (Δε +0.19 in MeOH) and 252 nm (Δε +0.19 in MeOH) for the 8*S* configuration in the α-methylene-γ-lactone, respectively. On the other hand, the CD data for **4** and **5** showed negative Cotton effects at 257 nm (Δε **4**: -0.34, **5**: -0.45 in MeOH), so that the absolute configurations of the 8-position were determined to be both *R*. Furthermore, the absolute configurations of the 2- and 4-positions were characterized by the application of a modified Mosher's method. Namely, treatment of **4** with (-)-α-methoxy-α-(trifluoromethyl)phenylacetyl chloride [(-)-MTPA-Cl] in pyridine yielded a mixture of (*S*)-MTPA esters, **8a** and **9a** (4:3),¹⁷ by intramolecular acetate transfer. Whereas, the (*R*)-MTPA esters, **8b** and **9b** (4:3), were derived from **4** by treatment with (+)-MTPA-Cl in pyridine. As shown in Fig. 4, the signals due to the protons attached to the 4 and 15-positions were observed at higher fields in the (*S*)-MTPA ester (**8a**) compared with the (*R*)-MTPA ester (**8b**) [Δδ: negative], while the signals due to the protons of the 5 and 14-positions were observed at lower fields in **8a** than **8b** [Δδ: positive]. Furthermore, the signal due to the proton attached to the 15-position was observed at higher fields in the (*S*)-MTPA ester (**9a**) than (*R*)-MTPA ester (**9b**) [Δδ: negative], while the signals due to the protons of the 2, 5 and 14-positions were observed at lower fields in **9a** than **9b** [Δδ: positive]. Thus the absolute configurations of the 2- and 4-positions of **4** were determined to be both *S* orientations. In the same manner, treatment of **5** with (-)-MTPA-Cl in pyridine yielded a mixture of (*S*)-MTPA esters, **8a** and **9a** (5:4). Whereas, the (*R*)-MTPA esters, **8b** and **9b** (5:4), were derived from **5**. Therefore, the absolute configurations of the 2- and 4-positions in **5** were clarified to be also both *S*. Finally, treatment of **4** and **5** with

Table 2. Inhibitory Effects of 1–7 and CAPE on NO Production in LPS-Stimulated RAW264.7 Cells

Inhibition (%)	Concentration of test sample (μM)							IC ₅₀ (μM)
	0	1	2	3	6	10	30	
5 α -Hydroperoxyvalin (1)	0.0 \pm 2.2	6.1 \pm 1.7	—	9.8 \pm 1.6**	20.3 \pm 1.2**	32.4 \pm 1.9** (107.1 \pm 2.0)	94.3 \pm 1.3** (87.8 \pm 2.8)	15.7
Ivalin (2)	0.0 \pm 1.7	15.0 \pm 1.0** (92.4 \pm 5.1)	46.7 \pm 0.7** ^(a) (72.3 \pm 3.7)	74.1 \pm 1.6** ^(a) (65.3 \pm 4.5)	98.8 \pm 0.1** ^(a) (43.9 \pm 4.9)	—	—	2.0
2 α -Hydroxylantolactone (3)	0.0 \pm 1.0	22.5 \pm 1.7** (95.8 \pm 1.1)	59.1 \pm 1.5** (77.1 \pm 0.9) ^(a)	87.9 \pm 1.6** ^(a) (63.8 \pm 0.9)	100.2 \pm 0.1** ^(a) (45.4 \pm 0.7)	—	—	1.8
8- <i>epi</i> -Xanthanol (4)	0.0 \pm 0.5	-2.7 \pm 1.1	—	1.1 \pm 2.2	-0.5 \pm 1.2	10.8 \pm 3.3** (102.3 \pm 1.7)	67.6 \pm 1.6** (98.2 \pm 4.9)	ca. 24
8- <i>epi</i> -Isoxanthanol (5)	0.0 \pm 1.7	7.0 \pm 1.1	—	10.0 \pm 2.6**	17.7 \pm 2.0**	31.2 \pm 0.4** (104.8 \pm 3.0)	76.5 \pm 0.8** (100.1 \pm 4.2)	18.9
Xanthanol (6)	0.0 \pm 0.4	0.2 \pm 2.2	—	11.5 \pm 2.1**	17.2 \pm 0.8**	30.4 \pm 0.6** (102.8 \pm 5.80)	96.4 \pm 0.6** (81.0 \pm 2.4)	15.8
Isoxanthanol (7)	0.0 \pm 1.1	12.8 \pm 1.7*	—	9.5 \pm 1.0**	16.5 \pm 1.1**	31.5 \pm 0.3** (101.8 \pm 3.3)	108.6 \pm 3.1** (4.5 \pm 2.2) ^(a)	14
α -Methylene- γ -lactone	0.0 \pm 1.2	9.8 \pm 0.5**	—	16.0 \pm 0.7**	—	31.1 \pm 0.7** (100.1 \pm 2.4)	60.1 \pm 0.6** (102.6 \pm 1.1)	22.8
Parthenolide	0.0 \pm 1.1	29.3 \pm 0.5** (103.5 \pm 5.3)	—	74.8 \pm 0.2** ^(a) (40.0 \pm 0.6)	—	99.6 \pm 0.2** ^(a) (0.9 \pm 0.0)	—	ca. 1.1
CAPE	0.0 \pm 0.7	13.4 \pm 0.8**	—	37.8 \pm 0.7** (86.8 \pm 1.6)	84.7 \pm 0.9**	95.9 \pm 0.8** (22.0 \pm 0.6) ^(a)	—	3.5

Values represent the mean \pm S.E.M. ($n=4$). Significantly different from the control (0 μM), * $p<0.05$, ** $p<0.01$. ^(a) A cytotoxic effect was observed, and values in parentheses indicate cell viability (%) in the MTT assay.

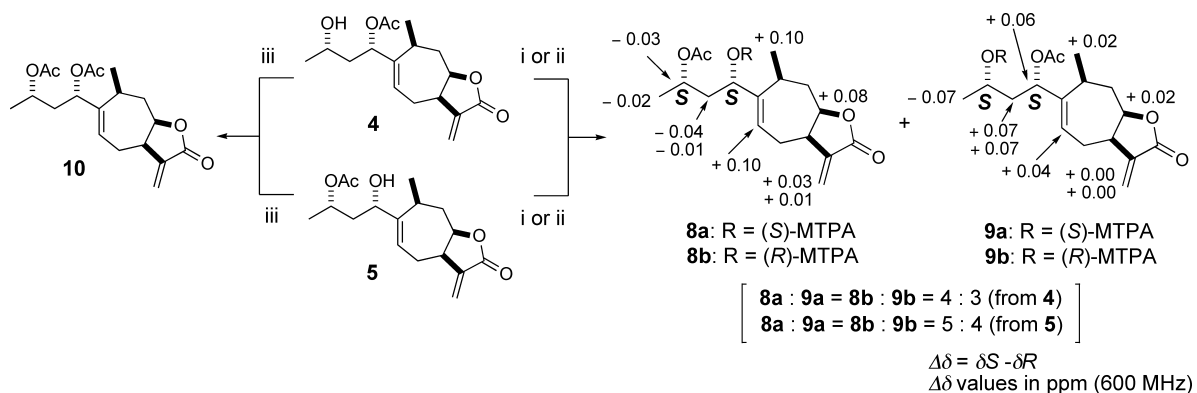


Fig. 4 Determination of the Absolute Configurations of 2- and 4-Positions on 4 and 5

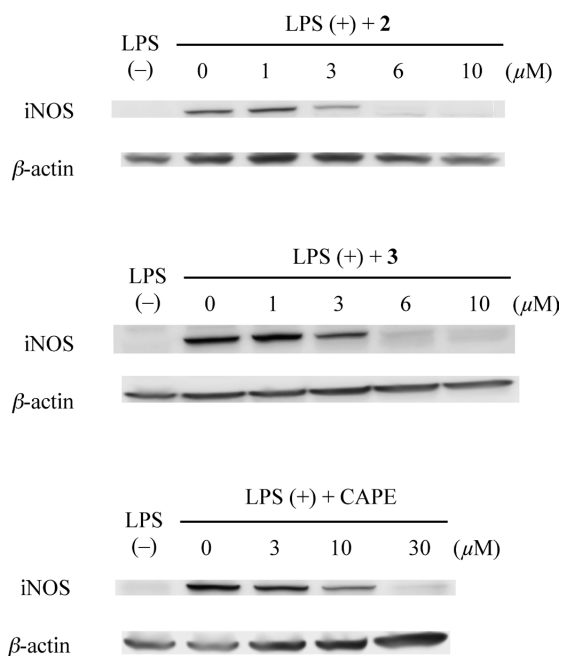


Fig. 5. Inhibitory Effects of 2, 3, and CAPE on Induction of iNOS in LPS-Stimulated RAW264.7 Cells

Ac₂O and pyridine furnished the same diacetate compound, **10**. Consequently, the structure of 8-*epi*-xanthanol (**4**) and 8-*epi*-isoxanthanol (**5**) was determined as shown.

Effects of 1–7 on Production of NO in RAW264.7 Cells
 In murine macrophage RAW264.7 cells, LPS alone induces the transcription and protein synthesis of iNOS, and increased NO production. Using the Griess reaction, a spectrophotometric determination of nitrite (NO₂[–]) was carried out to quantify levels in the conditioned medium of RAW264.7 cells treated with LPS. This cell-based assay system has been used for drug screening and the evaluation of potential inhibitors of the pathways leading to the induction of iNOS and NO production. Our results showed that all compounds (**1**–**7**) significantly inhibited NO production in LPS-activated RAW264.7 cells (Table 2). Ivalin (**2**) and 2 α -hydroxyalantolactone (**3**) showed the stronger inhibitory effects with IC₅₀ values of 2.0 and 1.8 μM, but stronger cytotoxic effects also. The reference compounds, caffeic acid phenethyl ester (CAPE) and parthenolide, exhibited strong inhibitory effects with IC₅₀ values of 3.5 μM and *ca.* 1.1 μM, respectively, together with cytotoxic

effects. Furthermore, effects of **2**, **3**, and CAPE on the induction of iNOS were examined using a sodium dodecyl sulfate-polyacrylamide gel electrophoresis (SDS-PAGE) Western-blot analysis. As shown in Fig. 5, **2** and **3** concentration-dependently inhibited iNOS protein production in RAW264.7 cells.

Recent studies have demonstrated that sesquiterpenes with an α -methylene- γ -lactone moiety (*e.g.* parthenolide, costunolide, and dhydrocostuslactone) to have inhibitory effects on nuclear factor-kappa B (NF- κ B) activation, and thereby iNOS expression following the inhibition of NO production in LPS-stimulated mouse peritoneal macrophages and RAW264.7 cells, and that the α -methylene- γ -lactone moiety is essential for strong activity.^{18–21} In the present study using RAW264.7 cells, eudesman-type sesquiterpenes, **2** and **3**, also showed strong inhibitory effects, but **1** having a hydroperoxide group and guaianolide-type sesquiterpenes (**4**–**7**) showed moderate inhibition (IC₅₀ of 14–24 μM) and weaker cytotoxic effects. The IC₅₀ values of **1** and **4**–**7** were similar to that of α -methylene- γ -lactone (IC₅₀=22.8 μM). These findings confirm that not only the α -methylene- γ -lactone structure but also other structures are important for strong inhibition. The structure–activity relationships of this type of sesquiterpene, excluding the lactone ring, should be studied further.

Experimental

General Experimental Procedures The following instruments were used to obtain physical data: specific rotations, a Horiba SEPA-300 digital polarimeter (*l*=5 cm); IR spectra, a Shimadzu FTIR-8100 spectrometer; CD spectra, a JASCO J-720WI spectrometer; CI-MS, electron ionization (EI)-MS and HR-CI-MS, a JEOL JMS-GCMATE mass spectrometer; FAB-MS and HR-FAB-MS, a JEOL JMS-SX 102A mass spectrometer; ¹H-NMR spectra, JEOL JNM-ECA600 (600 MHz) spectrometers; ¹³C-NMR spectra, JEOL JNM-ECA600 (150 MHz) spectrometers with tetramethylsilane as an internal standard; and HPLC, a Shimadzu RID-10A refractive index detector and YMC-Pack ODS-A (YMC, Inc., 250×4.6 mm i.d.) and (250×20 mm i.d.) columns for analytical and preparative purposes, respectively. The following experimental materials were used for chromatography: normal-phase silica gel column chromatography, Silica gel BW-200 (Fuji Silysia Chemical, Ltd., 150–350 mesh); reversed-phase silica gel column chromatography, Chromatorex ODS DM1020T (Fuji Silysia Chemical, Ltd., 100–200 mesh); TLC, precoated TLC plates with Silica gel 60F₂₅₄ (Merck, 0.25 mm) (ordinary

phase) and Silica gel RP-18 F_{254S} (Merck, 0.25 mm) (reversed phase); and reversed-phase HPTLC, precoated TLC plates with Silica gel RP-18 WF_{254S} (Merck, 0.25 mm). Detection was achieved by spraying with 1% Ce(SO₄)₂-10% aqueous H₂SO₄ followed by heating.

Plant Material The air-dried aerial parts of *Pulicaria undulata* (L.) KOSTEL were collected in June 2010, from North Sinia, Egypt. A voucher specimen, SK-103, has been deposited in the Herbarium of St. Katherine protectorate, Egypt.

Extraction and Isolation The aerial parts (1.8 kg) of *P. undulata* were powdered and extracted with CH₂Cl₂-MeOH (1:1) at room temperature. The extract was concentrated *in vacuo* to obtain a residue of 122 g (6.77%). The residue was fractionated on a silica gel column (6×120 cm) eluted with *n*-hexane (3000 mL) followed by a gradient of *n*-hexane-CHCl₃ up to 100% CHCl₃ and CHCl₃-MeOH up to 50% MeOH (3000 mL each of the solvent mixture). The *n*-hexane-CHCl₃ (1:3) fraction (22 g) was chromatographed on a Sephadex LH-20 column (3×90 cm) eluted with *n*-hexane-CH₂Cl₂-methanol (7:4:0.25). Fractions were obtained and combined into three main subfractions A, B, and C. Sub-fraction A (7 g) was re-purified by reversed-phase HPLC using MeOH/H₂O (55—45%) to afford compounds **4** (23 mg, 0.0013%), **5** (40 mg, 0.0022%), **6** (16 mg, 0.0009%), and **7** (65 mg, 0.0036%). Sub-fraction B (13 g) was re-purified by using silica gel column (6×90 cm) eluted with *n*-hexane-EtOAc (4:1) followed by reversed-phase HPLC using MeOH/H₂O (55—45%) to afford compounds **2** (22 mg, 0.0012%) and **3** (300 mg, 0.017%). Sub-fraction C (2 g) was re-purified by reversed-phase HPLC using MeOH/H₂O (60—40%) to afford **1** (7 mg, 0.0004%).

5 α -Hydroperoxyvalin (1): Colorless needles; mp. 218.0—220.0°C (recrystallized from CHCl₃-MeOH); [α]_D²⁵ +22.0° (*c*=0.5, MeOH); IR (KBr) ν_{\max} 3450, 2926, 1735, 1650 cm⁻¹; ¹H-NMR data see Table 1; ¹³C-NMR data see Table 1; FAB-MS *m/z* 303 [M+Na]⁺; HR-FAB-MS: *m/z* 303.1204 (Calcd for C₁₅H₂₀O₅Na [M+Na]⁺, 303.1208).

8-*epi*-Xanthanol (4): Colorless oil; [α]_D²⁵ -15.0° (*c*=1.0, MeOH); IR (KBr) ν_{\max} 3450, 1738, 1732, and 1652 cm⁻¹; ¹H-NMR data see Table 1; ¹³C-NMR data see Table 1; CI-MS *m/z* 309 [M+H]⁺; HR-CI-MS: *m/z* 309.1705 (Calcd for C₁₇H₂₅O₅ [M+H]⁺, 309.1702).

8-*epi*-Isoxanthanol (5): Colorless oil; [α]_D²⁵ -22.0° (*c*=1.0, MeOH); IR (KBr) ν_{\max} 3450, 1738, 1732, and 1652 cm⁻¹; ¹H-NMR data see Table 1; ¹³C-NMR data see Table 1; CI-MS *m/z* 309 [M+H]⁺; HR-CI-MS: *m/z* 309.1705 (Calcd for C₁₇H₂₅O₅ [M+H]⁺, 309.1702).

Preparation of the (S)- and (R)-MTPA Esters (8a,b, 9a,b) from 4 A solution of **4** (3 mg, 0.01 mmol) in pyridine (0.5 mL) was treated with (-)-MTPA-Cl (0.01 mL, 0.066 mmol), and the mixture was stirred at r.t. for 12 h. The reaction mixture was poured into H₂O and extracted with EtOAc. The EtOAc extract was dried over Na₂SO₄ powder and filtered. Removal of the solvent from the filtrate under reduced pressure furnished a residue, which was purified by normal-phase silica gel column chromatography [*n*-hexane-EtOAc (2:1, v/v)] to give the mixture of (S)-MTPA ester derivatives, **8a** and **9a** (4.6 mg, 4:3). Through a similar procedure, the mixture of (R)-MTPA ester derivatives, **8b** and **9b** (4.5 mg, 4:3), was obtained from **4** (3.0 mg, 0.01 mmol) using (+)-MTPA-Cl.

2-(S)-MTPA Ester Derivative (8a): ¹H-NMR (CDCl₃,

600 MHz) δ : 1.05 (3H, d, *J*=6.9 Hz, H₃-14), 1.21 (3H, d, *J*=6.2 Hz, H₃-15), 1.80, 2.10 (1H each, both m, H₂-3), 2.03 (3H, s, CH₃CO-), 4.58 (1H, m, H-8), 4.81 (1H, m, H-4), 5.23 (1H, dd, *J*=6.2, 8.2 Hz, H-2), 5.54, 6.28 (1H each, both d, *J*=2.8 Hz, H₂-13), 5.84 (1H, dd, *J*=5.5, 9.6 Hz, H-5).

2-(R)-MTPA Ester Derivative (8b): ¹H-NMR (CDCl₃, 600 MHz) δ : 0.95 (3H, d, *J*=6.8 Hz, H₃-14), 1.23 (3H, d, *J*=6.2 Hz, H₃-15), 1.84, 2.11 (1H each, both m, H₂-3), 2.03 (3H, s, CH₃CO-), 4.50 (1H, m, H-8), 4.84 (1H, m, H-4), 5.24 (1H, dd, *J*=5.5, 7.6 Hz, H-2), 5.51, 6.27 (1H each, both d, *J*=2.8 Hz, H₂-13), 5.74 (1H, m, H-5).

4-(S)-MTPA Ester Derivative (9a): ¹H-NMR (CDCl₃, 600 MHz) δ : 1.10 (3H, d, *J*=6.9 Hz, H₃-14), 1.29 (3H, d, *J*=6.2 Hz, H₃-15), 1.84, 2.15 (1H each, both m, H₂-3), 2.03 (3H, s, CH₃CO-), 4.62 (1H, m, H-8), 5.05 (1H, dd, *J*=5.5, 8.9 Hz, H-2), 5.11 (1H, m, H-4), 5.54, 6.28 (1H each, both d, *J*=2.8 Hz, H₂-13), 5.78 (1H, dd, *J*=6.2, 9.6 Hz, H-5).

4-(R)-MTPA Ester Derivative (9b): ¹H-NMR (CDCl₃, 600 MHz) δ : 1.08 (3H, d, *J*=6.9 Hz, H₃-14), 1.36 (3H, d, *J*=6.2 Hz, H₃-15), 1.77, 2.08 (1H each, both m, H₂-3), 2.03 (3H, s, CH₃CO-), 4.60 (1H, m, H-8), 4.99 (1H, dd, *J*=4.8, 8.2 Hz, H-2), 5.10 (1H, m, H-4), 5.54, 6.28 (1H each, both d, *J*=2.8 Hz, H₂-13), 5.74 (1H, m, H-5).

Preparation of the (S)- and (R)-MTPA Esters (8a,b, 9a,b) from 5 The mixture of (S)-MTPA ester derivatives, **8a** and **9a** (4.5 mg, 5:4), and the mixture of (R)-MTPA ester derivatives, **8b** and **9b** (4.3 mg, 5:4), was each obtained from **5** (each 3.0 mg, 0.01 mmol) using a similar procedure to when MTPA ester derivatives were obtained from **4**.

Preparation of the Diacetate (10) from 4 and 5 A solution of **4** (3.0 mg, 0.01 mmol) in pyridine (0.5 mL) was treated with Ac₂O (0.5 mL), and the mixture was stirred at rt for 12 h. The reaction mixture was poured into H₂O and extracted with EtOAc. The EtOAc extract was dried over Na₂SO₄ powder and filtered. Removal of the solvent from the filtrate under reduced pressure furnished a residue, which was purified by normal-phase silica gel column chromatography [*n*-hexane-EtOAc (2:1, v/v)] to give **10** (3.2 mg). Through the same procedure, diacetate (**10**, 3.0 mg) was obtained from **5** (3.0 mg, 0.01 mmol).

X-Ray Crystallography Data for 1 Single crystal X-ray analysis established the complete structure and relative configuration of **1**. The crystal data can be summarized as follows: C₁₅H₂₀O₅, formula wt 280.32, Orthorhombic, space group *P*₂₁₂₁, *a*=9.6395 (2) Å, *b*=11.0925 (2) Å, *c*=13.0510 (2) Å, *V*=1395.49 (5) Å³, *Z*=4, *D*_{cacl}=1.334 g/cm³, crystal size 0.369×0.344×0.267 mm³. All diagrams and calculations were performed using Rigaku R-Axis RAPID diffractometer, with graphite monochromated CuK α radiation (λ =1.54187 Å). The structures were refined by full matrix least squares on *F*² using Bruker SHELX-97.²²⁾ The final *R* and *R*_w were 0.0409 and 0.0888, respectively.

Bioassay Method. Cell Culture The murine macrophage cells (RAW264.7, ATCC No. TIB-71) were obtained from Dainippon Pharmaceutical, Osaka, Japan and cultured in Dulbecco's modified Eagle's medium (DMEM, 4500 mg/L glucose) supplemented with 10% fetal calf serum, penicillin (100 U/mL), and streptomycin (100 μ g/mL) (Sigma Chemical Co., St. Louis, MO, U.S.A.). The cells were incubated at 37°C in 5% CO₂/air.

Effects on Production of NO in LPS-Stimulated RAW264.7 Macrophages The total amount of nitrite in a

medium is used as an indicator of NO synthesis. The screening test for NO production using RAW264.7 cells was described previously.²³⁾ Briefly, RAW264.7 cells were cultured in DMEM, and the suspension seeded into a 96-well microplate at 2.5×10^5 cells/100 μ L/well. After 6 h, nonadherent cells were removed by washing with phosphate buffered saline (PBS), the adherent cells were cultured in 100 μ L of fresh medium containing the test compounds for 10 min, and then 100 μ L of the medium containing LPS (from *E. coli*, 055: B5, Sigma) was added to stimulate the cells for 18 h (final concentration of LPS, 10 μ g/mL). The nitrite concentration was measured from the supernatant by a Griess reaction. NO production in each well was assessed by measuring the accumulation of nitrite in the culture medium using Griess reagent. Inhibition (%) was calculated using the following formula and the IC₅₀ was determined graphically ($n=4$).

$$\text{inhibition (\%)} = [(A - B) / (A - C)] \times 100$$

A-C: nitrite concentration (μ M). A: LPS (+), sample (-); B: LPS (+), sample (+); C: LPS (-), sample (-)

Determination of Cytotoxic Effects Cytotoxicity was evaluated by the 3-(4,5-dimethyl-2-thiazolyl)-2,5-diphenyl-2H-tetrazolium bromide (MTT) colorimetric assay according to a previous report with a slight modification.²³⁾ Briefly, RAW264.7 cells (1.0×10^5 cells/200 μ L/well) were incubated with test compounds without LPS for 18 h. An aliquot of the medium (100 μ L) was removed and MTT solution (10 μ L, 5 mg/mL in PBS) was then added. After a 2-h incubation at 37°C, the medium was removed, and isopropanol containing 0.04 M HCl was added to dissolve the formazan produced in the cells. The optical density (OD) of the formazan solution was measured with a microplate reader at 570 nm (reference: 655 nm). If the OD of the sample-treated group dropped below 80% of that in the vehicle-treated group, the test compound was considered cytotoxic.

SDS-PAGE and Western Blot Analysis The detection of iNOS was determined according to methods described previously.²³⁾ RAW 264.7 cells (5.0×10^6 cells/2 mL/well) were seeded into a 6-well multiplate and allowed to adhere for 6 h at 37°C in a humidified atmosphere containing 5% CO₂. The cells were then washed with PBS, 1 mL of DMEM containing various concentrations of the test samples was added to each well, and after incubation for 10 min, 1 mL of DMEM containing LPS was added to stimulate the cells for 12 h (final concentration of LPS was 10 μ g/mL). The adhered cells were collected using a cell scraper in a lysis buffer (15 mM NaCl, 1 mM Tris, 1.0% Triton-X, 0.2 mM ethylene glycol bis(2-aminoethylether)-*N,N,N',N'*-tetraacetic acid (EGTA), 2.8 mM β -glycerophosphate) containing protease inhibitor cocktail (Thermo Scientific) and phosphatase inhibitor cocktail (PhosSTOP, Roche). Cells were disrupted three times (Microson™ ultrasonic cell disruptor, U.S.A.) for 30 s, and centrifuged at 10000 rpm for 10 min. Protein concentrations of cell lysates were determined using the BCA™ protein assay kit (Thermo Scientific). For protein sample preparation, 100 μ L of supernatant was transferred to 100 μ L of a dissolving agent (0.9 mM EGTA, 200 mM SDS, 2.8 mM Tris, 8% glycerol, 0.03% bromophenol blue, 6% mercaptoethanol). The samples were heated in boiling water for 5 min. After cooling down, the samples were kept at -80°C until used.

A positive control, CAPE, and test samples were loaded

onto 10% SDS-polyacrylamide gels (BIO-RAD ready gel J). For the Western blot analysis, β -actin was used as an internal standard. After electrophoresis, the proteins from each experiment were transferred onto a polyvinylidene fluoride (PVDF) membrane (BIO-RAD, HC, U.S.A.). The membrane was then soaked in Tris-buffered saline containing 0.1% Tween 20 (T-TBS) with gentle shaking at 75 rpm for 10 min, three times. For the blocking of the nonspecific sites, the membrane was soaked in Blocking One (Nacalai Tesque, Japan) by shaking for 0.5 h. The membrane was rinsed with T-TBS and incubated with specific primary antibodies: iNOS and β -actin (1:1000, Cell Signaling Technology). After incubation 1 h at r.t., the membrane was rinsed in T-TBS, and incubated in secondary antibodies (horse-radish peroxidase (HRP)-conjugated goat anti-mouse and anti-rabbit immunoglobulin G (IgG), 1:5000) in an immunoreactions enhancer solution (Can Get Signal, Toyobo, Japan) for 1 h. Next, the membrane was shaken in T-TBS for 10 min, three times. The proteins were detected using an enhanced chemiluminescence (ECL) plus Western blotting detection system (Amersham™ GE Healthcare, Biosciences). The images of membranes were recorded using a luminescent image analyzer, LAS-4000 mini (FUJIFILM, Japan).

Statistical Analysis All data are expressed as the mean \pm S.E.M. The data analysis was performed with a one-way analysis of variance (1-ANOVA), followed by Dunnett's test. A *p* value of less than 0.05 was considered to be significant.

Acknowledgements The research described in this paper was supported by a JSPS (Japan Society for the Promotion of Science) postdoctoral fellowship (ID No. P10117).

References and Notes

- Williams C. A., Harborne J. B., Greenham J. R., Grayer R. J., Kite G. C., Eagles J., *Phytochemistry*, **64**, 275–283 (2003).
- Liu L.-L., Yang J.-L., Shi Y.-P., *Chem. Biodivers.*, **7**, 327–349 (2010).
- Stavri M., Mathew K. T., Gordon A., Shnyder S. D., Falconer R. A., Gibbons S., *Phytochemistry*, **69**, 1915–1918 (2008).
- MacMicking J., Xie Q. W., Nathan C., *Annu. Rev. Immunol.*, **15**, 323–350 (1997).
- Lala P. K., Chakraborty C., *Lancet Oncol.*, **2**, 149–156 (2001).
- Murakami A., *Forum Nutr.*, **61**, 193–203 (2009).
- Hiraku Y., Kawanishi S., Ichinose T., Murata M., *Ann. N. Y. Acad. Sci.*, **1203**, 15–22 (2010).
- Inhibition (%) of the extract at 1, 3, 10, and 30 μ g/mL were 13.7 ± 2.5 , 43.4 ± 1.4 ($p < 0.01$), 80.4 ± 0.8 ($p < 0.01$), and 86.1 ± 0.31 ($p < 0.01$), respectively.
- Topcu G., Oksuz S., Shieh H. L., Cordell G. A., Pezzuto J. M., Bozok-Johansson C., *Phytochemistry*, **33**, 407–410 (1993).
- Herz W., Hoegenauer G., *J. Org. Chem.*, **27**, 905–910 (1962).
- Al-Yahaya M. A., Khafagy S., Shihata A., Kozlowski J. F., Antoun M. D., Cassady J. M., *J. Nat. Prod.*, **47**, 1013–1017 (1984).
- Marco J. A., Sanz-Cervera J. F., Corral J., Carda M., Jakupovic J., *Phytochemistry*, **34**, 1569–1576 (1993).
- Bohlmann F., Knoll K. H., El-Emary N. A., *Phytochemistry*, **18**, 1231–1233 (1979).
- The ¹H- and ¹³C-NMR spectra of **1**, **4**, and **5** were assigned with the aid of distortionless enhancement by polarization transfer (DEPT), double quantum filter correlation spectroscopy (DQF COSY), heteronuclear multiple quantum coherence spectroscopy (HMQC), and heteronuclear multiple bond connectivity spectroscopy (HMBC) experiments.

- 15) Gawronski J. K., van Oeveren A., van der Deen H., Leung C. W., Feringa B. L., *J. Org. Chem.*, **61**, 1513—1515 (1996).
- 16) Stoecklin W., Waddell T. G., Geissman T. A., *Tetrahedron*, **26**, 2397—2409 (1970).
- 17) The ¹H-NMR spectra of **8a**, **8b**, **9a**, and **9b** were assigned with the aid of DEPT, DQF COSY, HMQC, and HMBC experiments.
- 18) Matsuda H., Kagerura T., Toguchida I., Ueda H., Morikawa T., Yoshikawa M., *Life Sci.*, **66**, 2151—2157 (2000).
- 19) Matsuda H., Toguchida I., Ninomiya K., Kageura T., Morikawa T., Yoshikawa M., *Bioorg. Med. Chem.*, **11**, 709—715 (2003).
- 20) Koo T. H., Lee J. H., Park Y. J., Hong Y. S., Kim H. S., Kim K. W., Lee J. J., *Planta Med.*, **67**, 103—107 (2001).
- 21) Ríos J. L., Recio M. C., Escandell J. M., Andújar I., *Curr. Pharm. Des.*, **15**, 1212—1237 (2009).
- 22) Sheldrick G. M., *Acta Crystallogr.*, **A64**, 112—122 (2008).
- 23) Sae-Wong C., Matsuda H., Tewtrakul S., Tansakul P., Nakamura S., Nomura Y., Yoshikawa M., *J. Ethnopharmacol.*, **136**, 488—495 (2011).